Template Fabrication of Protein-Functionalized Gold−Polypyrrole−Gold Segmented Nanowires

Rose M. Hernández,[†,‡] Lee Richter,[‡] Steve Semancik,[‡] Stephan Stranick,[‡] and Thomas E. Mallouk*[,†]

Intercollege Graduate Program in Materials and Department of Chemistry, The Pennsylvania State University, University Park, Pennsylvania 16802, and National Institute of Standards and Technology, Chemical Science and Technology Laboratory (NIST, CSTL), Gaithersburg, Maryland 20899

Received March 5, 2004. Revised Manuscript Received June 4, 2004

Gold-capped, protein-modified polypyrrole (Ppy) nanowires were grown electrochemically using porous aluminum oxide as a template. The effects of the conditions of electrochemical synthesis on Ppy growth and protein (avidin or streptavidin) incorporation were studied. Streptavidin-modified nanowires grown at constant potential had better electrochemical properties and equilibrated faster when exposed to fluorescently labeled biotin than did nanowires grown by potential cycling. Solution pH had little effect on protein incorporation; however, higher pH provided slower but more reproducible growth rate of the Ppy segments. The best conditions for synthesis of streptavidin-modified Ppy nanowires were constant potential deposition at 0.75 V vs SCE in a phosphate buffer saline solution at pH 9. This method provides a straightforward route to nanowires of controlled length that can incorporate proteins for use in nanowire-based biosensors or in nanoparticle assembly through biomolecular interactions.

Introduction

Nanoparticles such as nanowires, nanotubes, and nanocrystals have been established as smart building blocks for emerging nanometer-sized electronic[1] and sensing devices.[2] Because of their very high aspect ratio, high electronic conductivity, and small size, nanowires and nanotubes offer potential advantages of high sensitivity, low power operation, and massive redundancy in nanosensor arrays. One challenge, however, is to devise ways in which appropriate molecular recognition elements can be incorporated. Nanowires and nanotubes modified with different proteins[3,4] and oligonucleotides[5,6] have recently been studied for the electronic detection of species of biological relevance. Lieber and co-workers[7] have made biosensors by aligning amine-modified silicon nanowires onto electrodes patterned on a silicon wafer to create a nanowire field effect transistor (FET). These derivatized nanowires were modified with biotin to produce sensors for streptavidin or an antibiotin antibody. Similarly, biosensors based on individual carbon nanotube FETs have recently been made by covalently linking proteins to the surface of nanotubes to impart chemical selectivity.[3] While these devices have shown excellent sensitivity, they rely on postsynthesis covalent modification of nanowires and nanotubes that can be difficult to produce, purify, and manipulate. Nanowires and nanotubes modified with biological molecules are also interesting building blocks for self-assembling nanostructures because very specific biomolecular interactions can be used to program their assembly.[6,8]

Polypyrrole (Ppy) is an interesting material for incorporation into nanowire-based sensors and nanostructures because of its high environmental stability, electronic conductivity, ion exchange capacity, and biocompatibility.[9] These properties have made Ppy a popular constituent of planar electrochemical biosensors.[10,11] Although several strategies for the synthesis of Ppy nanowires and nanotubes have been reported,[12,13] their applications as nanoscale biosensors are only beginning to be explored. Wallace and co-workers[14] recently developed a glucose sensor based on an array of carbon

* To whom correspondence should be addressed. Phone: 814-863-9637. Fax: 814-863-8403. E-mail: tom@chem.psu.edu.
† The Pennsylvania State University.
‡ NIST, CSTL.

(1) (a) Kovtyukhova, N. I.; Martin, B. R.; Mbindyo, J. K. N.; Smith, P. A.; Ravazi, B.; Mayer, T. S.; Mallouk, T. E. *J. Phys. Chem. B* **2001**, *105*, 8762. (b) Peña, D. J.; Mbindyo, J. K. N.; Carado, A. J.; Mallouk, T. E.; Keating, C. D.; Ravazi, B.; Mayer, T. S. *J. Phys. Chem. B* **2002**, *106*, 7458. (c) Cui, Y.; Zhong, Z.; Wang, D.; Wang, W. U.; Lieber, C. M. *Nano* Lett. **2002**, *3*, 149. (d) Zhong, Z.; Qian, F.; Wang, D.; Lieber, C. M. *Nano* Lett. **2003**, *3*, 343.

(2) (a) Suaud-Chagny, M. F.; Gonon, F. G. *Anal.* Chem. **1986**, *58*, 412. (b) Ebersole, R. C.; Miller, J. A.; Moran, J. R.; Ward, M. D. *J. Am.* Chem. Soc. **1990**, *112*, 3239. (c) Pantano, P.; Kuhr, W. G. *Anal.* Chem. **1993**, *65*, 623. (d) Hoshi, T.; Anzai, J.; Osa, T. *Anal.* Chem. **1995**, *67*, 770. (e) Feltus, A.; Ramanathan, S.; Daunert, S. *Anal. Bio*chem. **1997**, *254*, 62.

(3) (a) Star, A.; Gabriel, J. P.; Bradley, K.; GrUner, G. *Nano Lett.* **2003**, *3*, 639. (b) Besteman, K.; Lee, J.; Wiertz, F. G. M.; Heering, H. A.; Dekker, C. *Nano Lett.* **2003**, *3*, 727.

(4) Banerjee, I. A.; Yu, L.; Matsui, H. *Nano Lett.* **2003**, *3*, 283.

(5) Li, J.; Ng, H. T.; Cassell, A.; Fan, W.; Chen, H.; Ye, Q.; Koehne, J.; Han, J.; Meyyappan, M. *Nano Lett.* **2003**, *3*, 597.

(6) Reiss, B. D.; Mbyndyo, J. N. K.; Martin, B. R.; Nicewarner, S. R.; Mallouk, T. E.; Natan, M. J.; Keating, C. D. *MRS Symp. Proc.* **2001**, *635*, c6.2.1.

(7) Cui, Y.; Wei, Q.; Park, H.; Lieber, C. M. *Science* **2001**, *293*, 1289.

(8) (a) Sapp, S. A.; Mitchell, D. T.; Martin, C. R. *Chem. Mater.* **1999**, *11*, 1183. (b) Flynn, C. E.; Lee, S.-W.; Peelle, B. R.; Belcher, A. M. *Acta Mater.* **2003**, *51*, 5867.

10.1021/cm0496265 CCC: $27.50
Published on Web 08/07/2004

nanotubes coated with Ppy−glucose oxidase. The array constitutes a planar electrode with an extraordinary increase in surface area resulting from the polymer-coated nanotubes.

Martin et al.[13] have investigated the electrochemical and chemical template synthesis of Ppy within the pores of polycarbonate membranes. They prepared Ppy nanotubules of varying diameters and found higher conductivity than in Ppy thin films, which was attributed to alignment of polymer chains along the pore axis. Consequently, the study of structure−property relationships of conducting polymer nanostructures has become a subject of interest.[12] Other strategies for the fabrication of conducting polymer nanowires have entailed electrochemical synthesis on grafted insulating polymeric layers or on self-assembled monolayers.[15] While this method cleverly uses surface chemistry to direct the formation of nanowires, it lacks control over nanowire length, directionality, and dispersity. Recently, the self-assembly of Au/Ppy and Au/Ppy/Au nanowires into three-dimensional vesicle-like structures was reported.[16] These nanowires were synthesized using a similar approach to that described in this paper. However, our methods were modified to provide a biocompatible environment for incorporation of proteins.

We report the synthesis of segmented Au/(Ppy)/Au nanowires (300 nm in diameter and a few micrometers long) loaded with proteins in the polymer component as the first step toward the development of nanoscale biosensors and assemblies. We have studied some of the parameters (pH, monomer concentration, and electrochemical method of growth) that affect the growth of Ppy nanowires in a biocompatible environment to produce straight, monodisperse composite nanowires of desired lengths. These nanowires were made using anodic alumina templates in aqueous phosphate-buffered saline solutions (PBS) by two different electrochemical methods: constant potential and potential cycling. It is known that the choice of electrochemical method has an influence on the morphology, appearance, and adhesion of Ppy films.[17] Here, we show that the choice of method leads to differences in kinetic and mechanical behavior of the nanowires that are relevant to their use in sensors and self-assembling structures. Avidin and streptavidin were introduced into the nanowires by entrapment during Ppy polymerization,[11] and the effects of pH and electrodeposition potential on their incorporation were considered. The high specificity of the association between these proteins and biotin was used to monitor protein incorporation and accessibility in the conducting polymer segments of the nanowires as a function of the conditions of synthesis.

Experimental Section

Materials.[18] All electrochemical experiments were performed with a potentiostat/galvanostat (Princeton Applied Research, model 263A) in a one-compartment cell at room temperature. A Pt foil (2 cm^2) and a saturated calomel electrode (SCE) served as the counter electrode and reference electrode, respectively. Anodic alumina membranes (Whatman Inc., NJ) containing cylindrical pores ca. 0.3 μm in diameter were employed as the templates for nanowire growth. A thin layer (150 nm) of sacrificial Ag was deposited on the branched side of the membranes by thermal evaporation to serve as the working electrode. Pyrrole (98+%), $SnCl_2$ (99+%), $AgNO_3$ (100%), Na_2SO_3 (99.5%), formaldehyde (37%), 4-nitrophenyl phosphate disodium salt hexahydrate (97+%), and bovine serum albumin (BSA, 96+%) were obtained from Sigma. Methanol (99.96%), Na_2CO_3 (99.5%), and mercaptoacetic acid (98+%) were obtained from Aldrich. Aqueous ammonia (30%) and trifluoroacetic acid (neat) were obtained from J. T. Baker and Supelco, respectively. Au electroplating solution (Orotemp 24) and $Na_3Au(SO_3)_2$ (Oromerse Part B, 8×10^{-3} M) were obtained from Technic Inc., Cranston, RI. Avidin, streptavidin, avidin−rhodamine isothiocyanate (RITC), avidin−fluorescein isothiocyanate (FITC), streptavidin−FITC, biotin, and biotin−FITC were obtained from Molecular Probes (Eugene, OR). Biotinylated alkaline phosphatase was obtained from Pierce (Rockford, IL). Ultrapure water (18 MΩ-cm) was used for the preparation of all solutions and for rinsing. PBS solutions were prepared with 0.1 M NaCl (99.0%, Sigma), 0.003 M KCl (99.7%, J.T. Baker), and 0.002 M total phosphate concentration using potassium dihydrogen phosphate (99+%, Sigma) and disodium hydrogen phosphate (100%, J.T. Baker) to obtain pH values of 5.5, 7.4, and 8.8. HCl (37%, Aldrich) or NaOH (97+%, Aldrich) was added to obtain the lower and higher pH buffers.

Characterization.[18] Scanning electron microscope (SEM) images were obtained with a FEI-Phillips-Electroscan model 2020 environmental scanning electron microscope (E-SEM) and a field-emission scanning electron microscope (Hitachi S-4100 cold-cathode FE-SEM). Transmission electron microscope (TEM) images were obtained with a JEOL 1200 EXII at 80-kV accelerating voltage. Optical and fluorescence imaging was achieved with an Axiotech 100 reflected-light microscope (Carl Zeiss, NY) equipped with a CoolSNAP HQ camera (Roper Scientific, Inc., AZ). The light sources employed were an air-cooled argon-ion laser system (643 series, Melles Griot, CA) in dark field mode for fluorescence imaging and a tungsten lamp for optical imaging. Absorbance measurements were performed with a fiber optic spectrometer (Model SD2000, Ocean Optics, Inc., Dunedin, FL) equipped with tungsten−halogen and deuterium lamps (Model DT 1000 CE, Analytical Instrument System, Inc., Flemington, NJ).

Synthesis of Ppy Nanowires. A series of experiments were performed to determine the most favorable conditions for Ppy nanowire growth in PBS solutions, including the effect of pH, monomer concentration, and electrochemical method of polymerization. Solutions ranging from 0.05 to 1 M pyrrole, pH 7.4, were used to investigate the effect of monomer concentration on nanowire growth rate and homogeneity throughout the porous alumina membrane. As a result of this

(9) (a) Street, G. B.; Skotheim, T. A. *Handbook of Conducting Polymers*; Dekker: New York, 1986; Vol. 1, p 265. (b) Hailin, G.; Wallace, G. G. *Anal.* Chem. **1989**, *61*, 198. (c) Bieniarz, C.; Husain, M.; Tarcha, P. J. *Macromolecules* **1999**, *32*, 792. (d) Joo, J.; Lee, J. K.; Lee, S. Y.; Jang, K. S.; Oh, E. J.; Epstein, A. J. *Macromolecules* **2000**, *33*, 5131. (e) Yoshino, K.; Tada, K.; Yoshimoto, K.; Yoshida, M.; Kawai, T.; Araki, H.; Hamaguchi, M.; Zakhidov, A. *Synth.* Met. **1996**, *78*, 301. (f) Duchet, J.; Legras, R.; Demoustier-Champagne, S. *Synth.* Met. **1998**, *98*, 113. (g) Sadki, S.; Schottland, P.; Brodie, N.; Sabouraud, G. *Chem. Soc. Rev.* **2000**, *29*, 283.

(10) (a) Kryszewski, M. *Acta Phys.* Pol., A **1995**, *87*, 683.

(11) Cosnier, S. *Biosens. Bioelectron.* **1999**, *14*, 443.

(12) Duchet, J.; Legras, R.; Demoustier-Champagne, S. *Synth. Met.* **1998**, *98*, 113.

(13) (a) Martin, C. R. *Science* **1994**, *266*, 1961. (b) Martin, C. R. *Acc. Chem. Res.* **1995**, *28*, 61. (c) De Vito, S.; Martin, C. R. *Chem. Mater.* **1998**, *10*, 1738. (d) Penner, R. M.; Martin, C. R. *J. Electrochem. Soc.* **1986**, *133*, 2206.

(14) Gao, M.; Dai, L.; Wallace, G. G. *Synth. Met.* **2003**, *137*, 1393.

(15) (a) Jérôme, C.; Jérôme, R. *Angew. Chem., Int. Ed.* **1998**, *37*, 2488. (b) Choi, S.; Park, S. *Adv.* Mater. **2000**, *12*, 1547. (c) Jérôme, C.; Labaye, D.; Boart, I.; Jérôme, R. *Synth. Met.* **1999**, *101*, 3.

(16) Park, S.; Lim, J.; Chung, S.; Mirkin, C. A. *Science* **2004**, *303*, 348.

(17) Otero, T. F.; DeLaretta, E. *Synth. Met.* **1988**, *26*, 79.

(18) Disclaimer: Certain commercial equipment, instruments, or materials are identified in this report to specify adequately the experimental procedure. Such identification does not imply recommendation or endorsement by the National Institute of Standards and Technology, nor does it imply that the materials or equipment identified are necessarily the best available for the purpose.

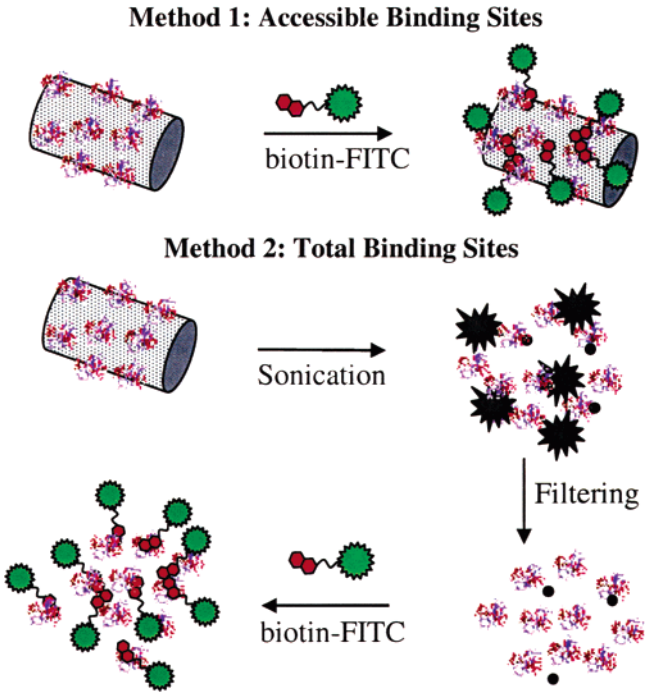

Figure 1. Schematic diagram of the methods used to quantify the amount of protein binding sites in Ppy nanowires.

preliminary optimization, Ppy nanowires were grown from 0.2 M pyrrole solutions in 150 mM PBS at pH 5.5, 7.4, and 8.8 for all other experiments. All solutions were bubbled with nitrogen immediately prior to use, and the electrochemical cell was protected from light to prevent monomer oxidation in solution. Although Ppy can be generated galvanostatically (0.48 mA/cm^2 current density), growth proved to be susceptible to gradients in the potential across the membrane, resulting in polydisperse wires. This problem was overcome by fixing the distance from the counter electrode to the alumina membrane at 2 cm for all experiments and by polymerizing at a constant potential (constant E) of +0.75 V or by E cycling between −0.2 and 0.9 V vs SCE at 20 mV/s. (Nanowires synthesized by constant E and E cycling are designated henceforth as Eco-nanowires and Ecy-nanowires, respectively.) The alumina membranes were subsequently treated with 25% (v/v) HNO_3 and 3 M sodium hydroxide to obtain free-standing particles. Nanowires were rinsed three times with water and three times with methanol and then re-suspended in methanol.

Incorporation of Avidin and Streptavidin into Ppy Nanowires. Immobilization of proteins into the Ppy matrix involved the physical entrapment of avidin, streptavidin, or their fluorescent conjugates during polymerization.[10,17,19] Protein-modified Ppy wires were grown from solutions containing 0.2 M pyrrole and 10 mg/mL of protein in PBS (pH 5.5, 7.4, and 9) at constant E of 0.75 V or by E cycling between −0.2 and 0.9 V vs SCE at 20 mV/s. The nanowires were rinsed with PBS solution of the same pH as polymerization solution and resuspended in PBS. A 1-mL sample of 10 mg/mL avidin-RITC in PBS was reacted with 300 μL of 10 mM D-bitoin in PBS prior to incorporation and was used to monitor the uptake of avidin in the Ppy segments of the nanowires by means of fluorescence imaging.

Protein Quantification. All nanowires used in this study were 320 ± 10 nm in diameter and 2 ± 0.2 μm long as determined by FE-SEM. Figure 1 illustrates the two methods used:

(1) Accessible Biotin Binding Sites. Binding assays were performed on protein-modified nanowires using standard biotin−FITC solutions (5−10 μM) in PBS at 25 °C, pH 7.4, for 10 h under constant agitation (in some cases binding assays were performed at different lengths of time). The amount of avidin or streptavidin entrapped in the nanowires was quantified by measuring the change in absorbance of the biotin−FITC stock solution at 494 nm before and after perfoming the binding assays. A 1-mL aliquot of stock solution containing (10^6 particles/mL) protein-modified nanowires was incubated with 0.5 mL of 10 μM biotin−FITC in PBS. The nanowire solution was centrifuged, and the nanowires were washed and resuspended in PBS (pH 7.4) for future experiments. Absorbance measurements were performed on the supernatant to determine the amount of biotin−FITC remaining in solution. The amount of biotin−FITC bound to the nanowires was calculated from the absorbance signal of the combined solutions and converted to the number of protein binding sites in the nanowires.

(2) Total Biotin Binding Sites. A modification of an indirect enzyme-linked binding assay method[20] was employed to estimate the total number of biotin binding sites per nanowire. The method is based on the fact that the reaction between an enzyme−biotin conjugate and avidin reduces the catalytic activity of the enzyme by altering its tertiary structure and/or because of steric effects. Avidin and streptavidin standard solutions were incubated with an excess amount of alkaline phosphatase−biotin conjugate and *p*-nitro-phenyl phosphate. The activity of biotinylated alkaline phosphatase was monitored from the absorbance at 405 nm of *p*-nitrophenol generated by the active enzyme. Aliquots of avidin or streptavidin were added to the binding assay, and calibration curves were generated by plotting the change in absorbance per unit time vs protein concentration. To quantify the number of binding sites in the protein-modified nanowires, the nanowires were sonicated to disrupt the Ppy matrix and to access buried protein molecules. As a control experiment, avidin and streptavidin standard solutions were sonicated for 1 min. This assay showed that 1-min sonication had little effect on the number of biotin binding sites in avidin or streptavidin samples. A 1-mL sample solution containing 10^7 protein-modified nanowires/mL was resuspended in an assay buffer containing 0.05 sodium carbonate (pH 9.4), 0.1 M NaCl, 0.01% (w/v) NaN_3, 0.01% (w/v) gelatin, and 0.2% (w/v) BSA. The samples were sonicated for 10 s, and the solutions were filtered with a PTFE filter (pore diameter ca. 0.2 μm) and incubated with excess biotinylated alkaline phosphatase for 10 min. A 50-μL aliquot of *p*-nitro-phenyl phosphate (20 mM) was added, and the absorbance of the samples was recorded over a 1-min period.

(3) Binding Kinetics of Biotin/Streptavidin. A suspension of 6.7 × 10^7 streptavidin-modified Ppy Eco-nanowires/mL prepared in PBS, pH 9, was reacted with 15 mM biotin−FITC at room temperature under constant stirring. Aliquots of 1 mL were drawn out periodically and reacted with excess unlabeled biotin to desorb any nonspecifically bound biotin−FITC molecules. The solutions were centrifuged for 20 min and the amount of unreacted biotin−FITC was determined from absorbance measurements of the supernatant. The amount of bound biotin−FITC was plotted as a function of incubation time. A suspension of 3.5 × 10^7 streptavidin-modified Ppy Ecy-nanowires/mL prepared in PBS, pH 9, was studied in the same way.

Synthesis of Segmented Au/Ppy/Au Nanowires. Electrodeposition of Au was done at a constant potential of −0.9 V vs SCE using a commercial Au plating solution. Au-containing membranes were soaked in pyrrole solutions for 10 min prior to polymerization. Ppy segments were electrodeposited as described above. The membrane-containing Au/Ppy was then immersed in 10 mM mercaptoacetic acid solution in methanol for 12 h. The second Au segment was grown by a slightly modified version of the electroless deposition method described by Menon and Martin.[21] The membranes were successively reacted at 25 °C with 0.025 M $SnCl_2$ and 0.07 M trifluoroacetic acid in 50:50 methanol/water (1 h), 0.03 M $AgNO_3$ in 0.3 M aqueous ammonia (10 min), and a solution

(19) Yang, Y.; Mu, S.; Chen, H. *Synth. Met.* **1998**, *92*, 173.

(20) Cho, H. C.; Lee, D. J.; Kim, S. Y.; Kim, J. H.; Paeng, I. R.; Cha, G. S. *Anal. Sci.* **1999**, *15*, 343.

(21) Menon, V. P.; Martín, C. R. *Anal. Chem.* **1995**, *67*, 1920.

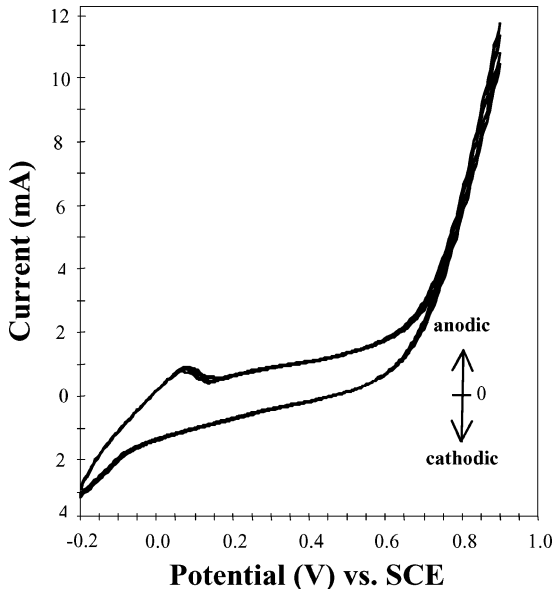

Figure 2. Cyclic voltammogram of Ppy Ecy-nanowire growth from 0.2 M pyrrole in PBS solution, pH 7.4. Scan started at −0.2 V; first four scans are shown, recorded at 20 mV/s.

containing 0.008 M $Na_3Au(SO_3)_2$/0.129 M Na_2SO_3/0.625 M HCHO adjusted to pH 10 (12 h) and then rinsed with copious amounts of methanol and water. The electrolessly deposited gold layers were elongated by electrochemical deposition of gold at a constant potential of −0.9 V vs SCE.

Results and Discussion

Effect of Growth Conditions on Ppy Nanowires: Morphology and Electrochemistry. *(1) Solvent and Monomer Concentration.* Figure 2 shows the cyclic voltammogram (CV) for the growth of Ppy nanowires by E cycling in PBS, pH 7.4, recorded at a scan rate of 20 mV/s. The steep rise in anodic current at 0.6−0.7 V corresponds to oxidation of the pyrrole monomer, whereas the cathodic and anodic peaks at −0.20 V and +0.05 V correspond to reduction and oxidation of the electrodeposited polymer. Because oxidation of the monomer occurs at a much higher potential than that of the polymer, side reactions including nucleophilic attack and overoxidation, and/or cross-linking of the polymer, should be expected. These reactions are potentially important, particularly in the incorporation of proteins that contain nucleophilic functional groups and in the derivitization of the polymer with thiol-containing molecules.

Aprotic solvents, such as acetonitrile, are known to be best for Ppy synthesis.[22] Unsworth et al. have shown that the adsorption of oxygen gas formed during water oxidation[23] is a source of surface defects in Ppy films regardless of any initial deoxygenation step. Pores created in this process may be desirable in terms of the permeability of analyte molecules; however, structural defects could deteriorate the electronic integrity of the nanowires. The rationale behind the electrochemical synthesis of Ppy is that when a Ppy monolayer is deposited on an electrode surface, it will be quickly

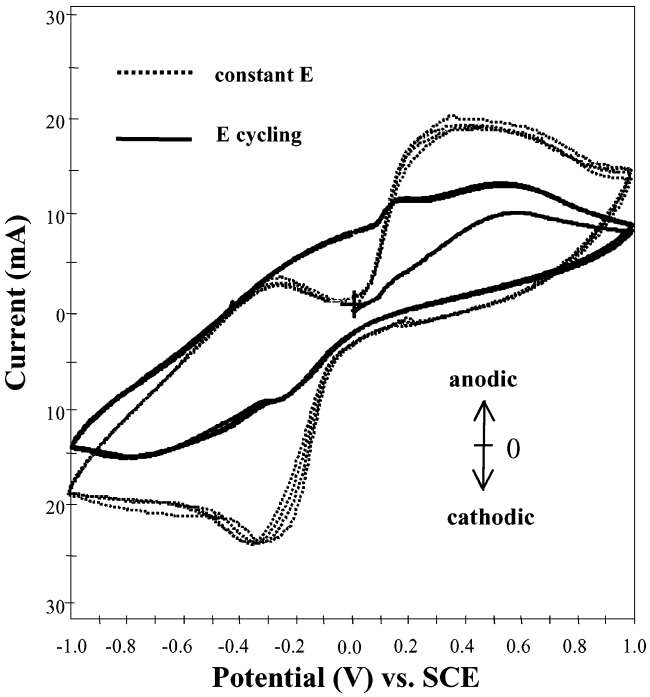

Figure 3. Cyclic voltammogram of Eco-nanowires and Ecy-nanowires embedded in the alumina template without protein modification, recorded at 100 mV/s in PBS, pH 7.4.

covered by a second monolayer. Simultaneously, the already deposited layers are subject to further oxidation (oxidative degradation). The rate of electrochemical oxidation of the deposited layers is dependent on the transport of counteranions through the layers. Previous chronoamperometric studies on Ppy films in aqueous solutions[24] considered the effects of chloride and phosphate as counterions. Electrodes prepared in chloride solution were in the electronically conductive oxidized state, and oxidation of monomers in solution could take place. In contrast, those electrodes prepared in phosphate solution were in the nonconductive neutral state. In our studies, both anions were present in solution with a chloride concentration 10-fold higher than phosphate's. Under these conditions, the effect of chloride ions appears to dominate, and both Ppy Eco- and Ecy-nanowires exhibited electroactivity (Figure 3).

The CV of membranes containing Eco- and Ecy-nanowires are compared in Figure 3. The CV of Eco-nanowires showed well-defined peaks characteristic of oxidation/reduction processes of polypyrrole films. Two anodic peaks at −0.3 and 0.35 V are associated with two oxidation processes that are normally observed in the presence of chloride ions.[24,25] A corresponding cathodic peak at −0.3 V was also observed. On the other hand, Ecy-nanowires showed smaller sharp anodic and cathodic peaks (indicative of slow charge-transfer diffusion or slow counterion diffusion in the polymer) superimposed on a background of broader anodic and cathodic waves. The latter is indicative of slow electron-transfer kinetics at the Ppy/solution interface. These characteristics are explained in later sections and may be associated with the differences in microstructure that

(22) Ko, J. M.; Rhee, H. W.; Park, S. M.; Kim, C. Y. *J. Electrochem. Soc.* **1990**, *137*, 905.
(23) Unsworth, J.; Innis, P. C.; Lunn, B. A.; Jin, Z.; Norton, G. P. *Synth. Met.* **1992**, *53*, 59.
(24) Zhao, S.; Luong, J. H. T. *Electroanalysis* **1995**, *7*, 633.
(25) van der Suijis, M. J.; Underhill, A. E.; Zaba, B. N. *J. Phys. D: Appl. Phys.* **1987**, *20*, 1411.

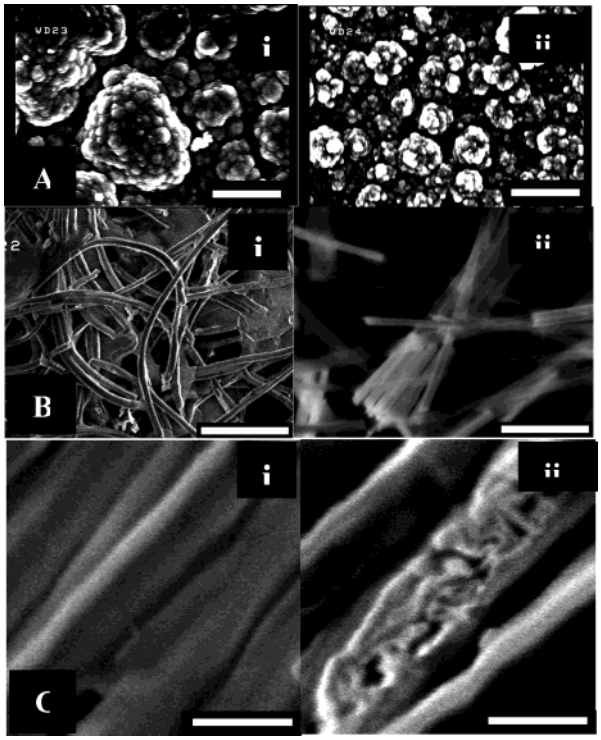

Figure 4. FE-SEM images of (A) Ppy films synthesized by (i) constant potential (0.75 V) and (ii) potential cycling (−0.2 to 0.8 V), scale bar 3 μm. (B) Difference in stiffness of (i) Eco-nanowires and (ii) Ecy-nanowires, scale bar 4.3 μm. (C) Structure of Eco-nanowires: (i) external and (ii) internal, scale bar 300 nm.

results from the growth of Ppy by the two different methods.

The concentration of pyrrole was varied from 0.05 to 1 M to determine the effect of monomer concentration on Ppy Eco-nanowire growth rate (data not shown). The growth rate increased with increasing monomer concentration; however, very polydisperse nanowire lengths were observed at low or high concentrations. We found that a concentration of 0.2 M gave good control [±4%] over nanowire length.

(2) Electrochemical Method of Synthesis. Ppy films were deposited onto 200-nm-thick gold-covered silicon substrates under the same experimental conditions used to grow Eco-nanowires and Ecy-nanowires. Electron micrographs of these films are shown in Figure 4a. As Zhou and Heinze pointed out,[26] the method of electrochemical synthesis controls the morphology of electrodeposited Ppy. Films obtained by E cycling were shiny black, with smaller grains, whereas larger "cauliflower" structures were formed with constant potential deposition.

A variation in the stiffness of nanowires synthesized by the two electrochemical methods was apparent when lengths exceeded 4 μm as illustrated in Figure 4b. Ecy-nanowires were straight even at lengths over 10 μm; in contrast, long Eco-nanowires were flexible and had spaghetti-like shapes after release from the alumina template. Figure 4c shows the external and internal morphology of a Ppy Eco-nanowire. The internal structure was revealed by agitating the nanowire solution to produce openings along the wire and was found to

(26) Zhou, M.; Heinze, J. *Electrochim. Acta* **1999**, *44*, 1733.

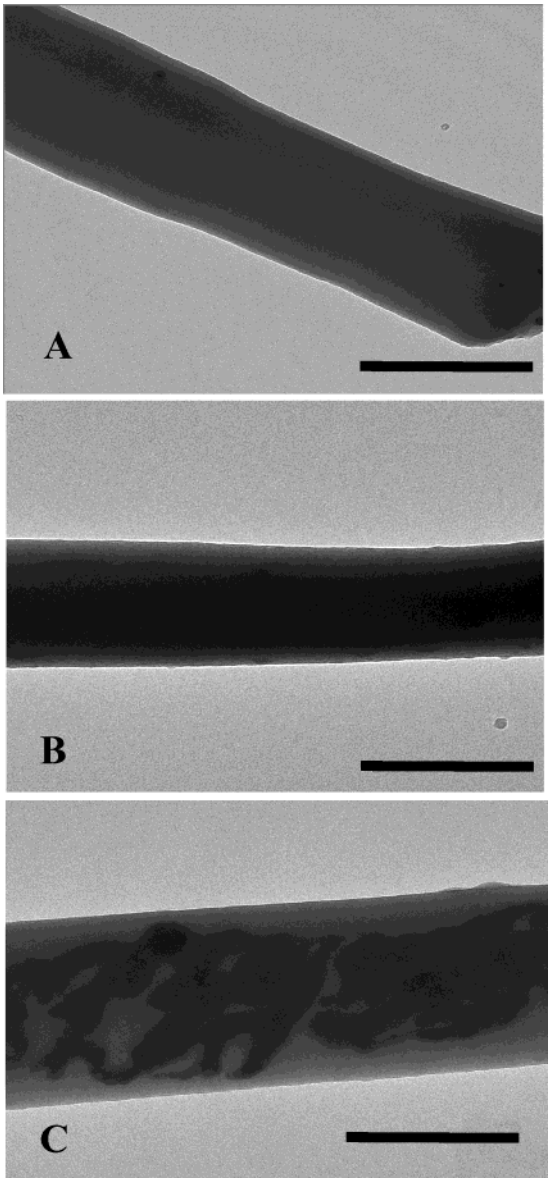

Figure 5. TEM images of (A) Ecy-nanowire and (B) Eco-nanowire, scale bar 250 nm. (C) Sodium chloride growth inside an Eco-nanowire, scale bar 200 nm.

be quite porous compared to the external surface. On the other hand, the stiffness of Ecy-nanowires made it imposible to produce open nanowires for imaging by simple agitation.

TEM images of Eco- and Ecy-nanowires are shown in Figure 5. These images confirm the synthesis of Ppy nanowires versus nanotubes. Structural differences between the two types of nanowires were not obvious (Figures 5a and 5b); however, TEM images such as that in Figure 5c were only found in some Eco-nanowires. The dark internal features in Figure 5c are consistent with the porosity observed in Figure 4c(ii). Such features could be due to the formation of salt crystals from pockets of PBS trapped in the Eco-nanowires. This characteristic was not observed in Ecy-nanowires, suggesting the absence of free volume inside Ecy-nanowires. Although both electrochemical methods yielded nanowires with smooth, featureless surfaces (consistent with polymer wetting of the pore walls of the template), the differences in their electrochemical behavior (Figure 3)

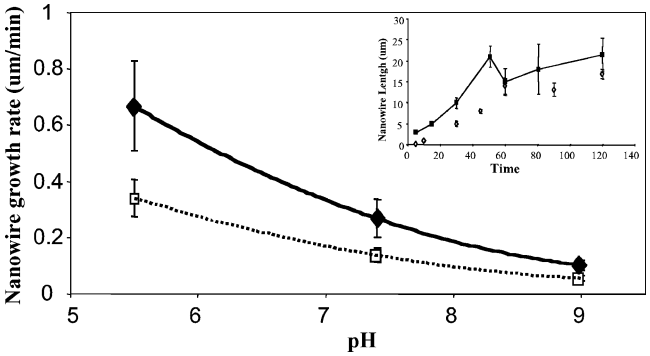

Figure 6. pH dependence of Ppy nanowire growth rate (μm/min). Nanowires synthesized by (□) E cycling (−0.2 to 0.9 V, 20 mV/s) and (◆) constant E (0.75 V). Inset: Eco-/Ecy-nanowire growth rate, pH 7.4.

and their rates of analyte adsorption (see below) are likely to result from differences in their internal structure.

(3) pH Dependence. Eco-nanowires and Ecy-nanowires were grown for various lengths of time and number of cycles, respectively. Faster growth is observed at lower pH, as shown in Figure 6. It is known that overoxidation of Ppy occurs more readily at higher pH and that significant nucleophilic attack occurs in aqueous solutions at pH ≥ 4.5.[27] However, for incorporation of proteins and other biomolecules into Ppy, it is necessary to find a compromise between biocompatible pH conditions and polymer stability.[28]

Protein Incorporation into Ppy Segments. Avidin and streptavidin were incorporated into Ppy nanowire segments by physical entrapment during electrodeposition. Figure 7 shows a bright field and corresponding fluorescence image of segmented Au/Eco-Ppy/Au nanowires modified with avidin−RITC excited at 488 nm. As expected, fluorescence was detected in the Ppy portion of the nanowires.

(1) Effect of Protein Charge. The effect of protein charge on incorporation into the Ppy nanowires was studied by varying the pH. The isoelectric points of avidin and streptavidin are 10 and 5 to 6, respectively. As a result, the net charges in avidin were positive and the net charges in streptavidin were negative, except at the low end of the pH range studied (pH 5.5) where streptavidin is near its isoelectric pH. Figure 8 shows that the amount of protein incorporated in Ppy nanowires does not have a significant pH dependence, even in the case of streptavidin near its isoelectric pH. Also, the difference between avidin and streptavidin incorporation is small at all values of pH. These results suggest that charge compensation of the cationic Ppy polymer is not the primary driving force for protein incorporation. Nucleophilic addition of reactive protein functional groups (NH_2, SH) at the surface of the growing Ppy segment[29] and hydrophobic protein−polypyrrole interactions[30] are other possible mechanisms for protein incorporation into the polymer. Two different

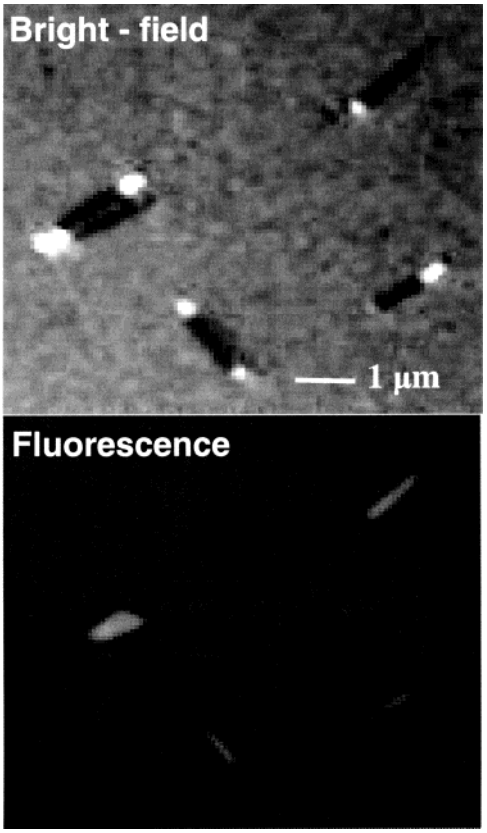

Figure 7. (a) Bright field and (b) fluoresce images of Au/Ppy/Au nanowires containing avidin−RITC in the Ppy matrix, excited at 488 nm, recorded at λ > 512 nm.

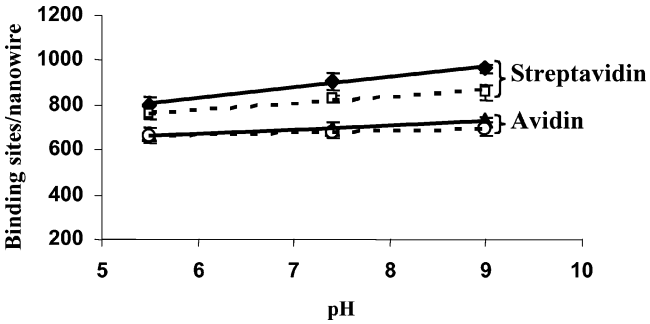

Figure 8. Binding sites in avidin/streptavidin-modified Ppy Eco-nanowires as a function of pH. Total binding sites in streptavidin (◆) and avidin (▲) modified nanowires; available binding sites after 10 h in streptavidin (□) and avidin (○) modified nanowires.

protein assays (see Figure 1) were used to obtain the data shown in Figure 8. The close correspondence between the total number of biotin binding sites and the number of binding sites that are accessible after 10 h in the intact wires indicates that essentially all the protein molecules incorporated are active (i.e., can bind biotin) given a sufficiently long equilibration time.

(2) Electrodeposition Potential. Eco-nanowires modified with avidin and streptavidin were grown at different potentials at pH 9. Figure 9 illustrates the amount of protein incorporated in the nanowires as a function of polymerization potential. Nanowires synthesized at constant 0.6 V contained more quantities of avidin and streptavidin than nanowires synthesized at constant 0.9 V. Polymerization at 0.9 V occurred relatively fast and may exceed the diffusion of proteins into the nanopores,

(27) Ghosh, S.; Bowmaker, G. A.; Cooney, R. P.; Seakins, J. M. *Synth. Met.* **1998**, *95*, 63.
(28) Kupila, E. L.; Kankare, J. *Synth.* Met. **1993**, *55*, 1402.
(29) Bieniarz, C.; Husain, M.; Tarcha, P. J. *Macromolecules* **1999**, *32*, 792.
(30) Azioune, A.; Chehimi, M. M.; Miksa, B.; Basinska, T.; Slomkowsky, S. *Langmuir* **2002**, *18*, 1150.

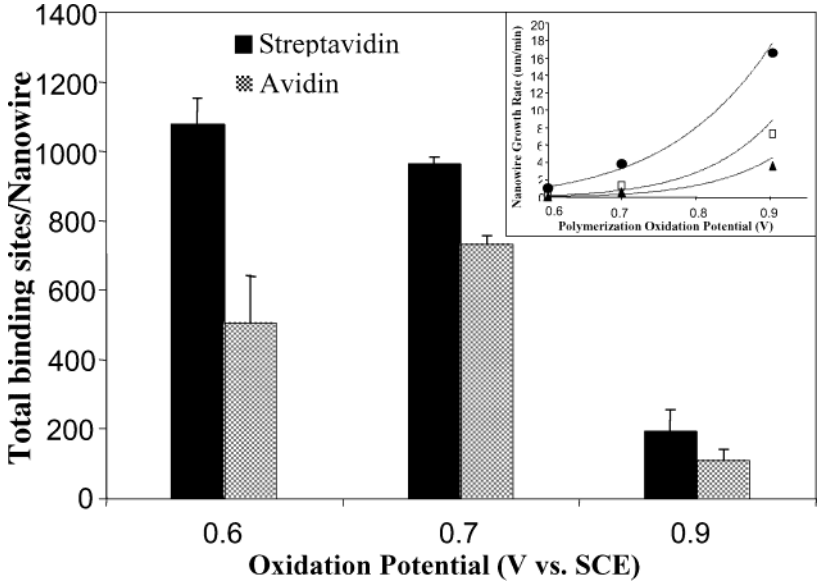

Figure 9. Streptavidin or avidin incorporated into nanowires synthesized at pH 9, as a function of constant oxidation potential. Inset: Growth rate as a function of oxidation potential for Eco-nanowires (no protein) grown at pH 5.5 (●), pH 7.4 (□), and pH 9 (▲).

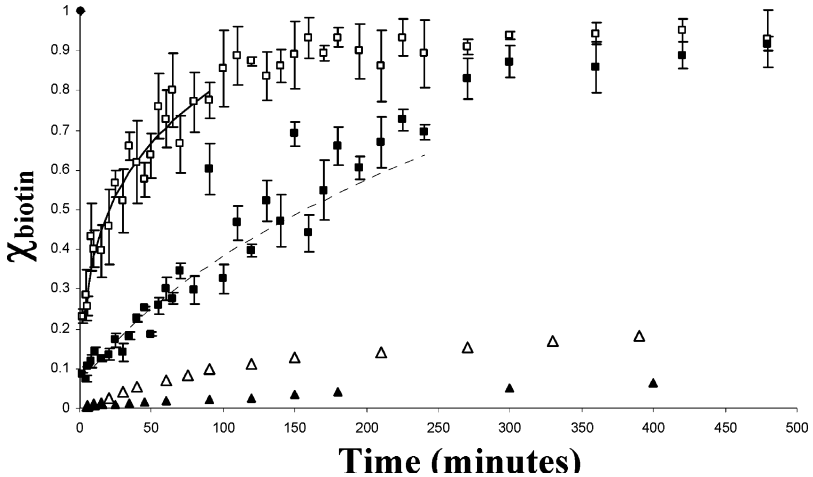

Figure 10. Adsorption kinetics for biotin−FITC binding to Ppy nanowires. Streptavidin−Ppy nanowires (□) and unmodified nanowires (△) synthesized by constant E. Streptavidin−Ppy nanowires (■) and unmodified nanowires (▲) synthesized by E cycling. Lines are best fits to eq 1.

yielding lower amounts of protein in the nanowires. At 0.6 V, polymerization is exceedingly slow (Figure 9, inset) and proteins are in equilibrium concentrations inside the nanopores.

(3) Binding Kinetics of Biotin / Streptavidin-Modified Nanowires. The amount of biotin−FITC bound or absorbed to streptavidin−Ppy nanowires (X_t) was measured as a function of time for nanowires made by constant E and E cycling, as shown in Figure 10. Here, saturation with biotin−FITC (X_s) was reached in approximately 100 and 300 min for Eco- and Ecy-nanowires, respectively. Biotin−FITC was also adsorbed onto Eco nanowires that contained no streptavidin, but the saturation coverage was only about 1/10 that of the streptavidin-modified nanowires. The kinetics of biotin−FITC uptake was studied using a thin film model originally developed to study the sorption and desorption of gases in polymers.[31] This model assumes that the sorption process is irreversible and that diffusion into the interior of the film is due to transport through the matrix. The approximation to the diffusion equation for this system is

$$X_t/X_s = 4/l\,[Dt/\pi]^{1/2} \qquad (1)$$

$$\chi_{\text{biotin}} \equiv X_t/X_s$$

where X_t is the total amount of biotin absorbed at time t, X_s is the amount corresponding to biotin saturation, l is the nanowire radius, and D is the effective diffusion coefficient. The lines in Figure 10 are best fits of eq 1 to the experimental data for $\chi_{\text{biotin}} < 80\%$, and D's are determined to be $5.4 \times 10^{-15} \pm$ cm^2/s and $1.2 \times 10^{-15} \pm$ cm^2/s for nanowires synthesized at constant E and E cycling, respectively. Nanowires synthesized at constant E have faster accessibility to the protein binding sites embedded in the Ppy matrix than those made by E cycling. This result is consistent with the cyclic voltammetry experiments (Figure 3), which showed evidence

(31) Vieth, W. R. *Diffusion In and Through Polymers: Principles and Aplications*; Oxford University Press: New York, 1991.

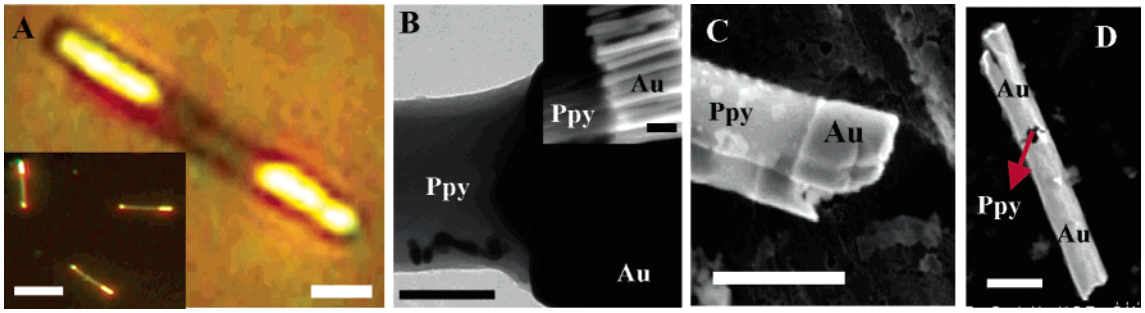

Figure 11. (A) Optical micrographs of an Au/Eco-Ppy/Au nanowire in bright-field mode, scale bar 1 μm. Diameter and total length are 314 nm and 4 μm, respectively. The inset shows a dark field image of small aspect ratio Au/Eco-Ppy/Au nanowire, scale bar 4 μm. (B) TEM image of Au/Eco-Ppy junction, scale bar 100 nm; the inset shows an ESEM micrograph of the same junctions, scale bar 1 μm. (C) FE-SEM micrograph of Au/Ppy junction after electroless deposition of second Au cap, scale bar 600 nm. (D) FE-SEM micrograph of an Au/Ppy/Au nanowire after electrochemical deposition of the second gold cap, scale bar 600 nm.

of slow mass transport of charge-compensating anions (which are small compared to biotin−FITC) in Ecy-nanowires. The faster diffusion of both electrochemical species and biotin conjugates in Eco-nanowires seems likely due to their open internal structure (Figure 4). Indeed, the differences in the internal structures of Eco- and Ecy-nanowires seem to play a significant role in the kinetic behavior of the Ppy nanowires.

Template Growth of Segmented Au/Ppy/Au Nanowires. Eco-nanowires were selected for the synthesis of segmented Au/Ppy/Au nanowires since their physical, electrochemical, and kinetic properties proved to be more suitable for biosensing applications than Ecy-nanowires. Au/Ppy/Au nanowires were made by successive electrodeposition of Au, electropolymerization of Ppy at constant E, and electroless gold deposition (Figure 11A). Ppy segments were capped with gold at each end to facilitate electrofluidic alignment[32] and to allow for low resistance contacts in subsequent electrical measurements. Good physical contact and sharp junctions between the Ppy segment and the top gold segments of the nanowires could be achieved by following an electroless plating procedure in which the exposed Ppy was first exposed to mercaptoacetic acid. The purpose of this step was the nucleophilic addition of thiol groups to the Ppy surface to create reactive carboxylate functionality for electroless deposition of gold.[29] Sn(II) was complexed by the carboxylate groups by immersion of the membrane in $SnCl_2$ solution, and Ag nanoparticles were then deposited via reaction of Sn(II) with Ag(I). After thorough rinsing with methanol and water, Au was then electrolessly deposited from a solution containing $Na_3Au(SO_3)_2$, Na_2SO_3, and formaldehyde.

The initial Au/Ppy junction produced by the electrochemical deposition of Au, followed by electropolymerization of Eco-Ppy (Figure 11B), yielded smooth and strong junctions. Au/Eco-Ppy nanowires were capped by two different methods: electroless deposition of Au as described above and direct electrochemical deposition of Au on Ppy. Ppy/Au junctions obtained by these two methods were quite different in structure as seen in Figures 11C and 11D. The electroless gold top contacts did not appear to penetrate the Ppy segments significantly (Figure 11C). On the other hand, electrodeposited gold permeated the Ppy segments of Eco-nanowires, leading to very poorly defined junctions and in many cases physical contact (electrical short) between the top and bottom Au segments (Figure 11D). We explain this phenomenon in terms of electrostatic interactions between ionic species and the polymer matrix. The electrodeposited Ppy is cationic and should exchange anions with contacting solutions. In the case of the electroless Au plating bath, the anion in highest concentration is SO_3^{2-}, which is likely to compete effectively with $[Au(SO_3)_2]^{3-}$ for ion-exchange sites in the polymer. The Au electroplating solution contains both $[Au(CN)_2]^-$ and CN^- anions. It is possible that $[Au(CN)_2]^-$ ions exchange into the polymer and that this leads to deposition of metallic gold throughout the polymer matrix rather than just at the tip. Therefore, an electroless deposition method was required for capping the Ppy segments. Finaly, the top Au cap was extended by further electrochemical deposition of Au to produce segmented nanowires as shown in Figure 11A.

Conclusions

The electrochemical replication of porous alumina membranes provides a straightforward route to free-standing nanowires of controlled length and functionality. Because they are easily modified chemically, conducting polymer segments in these nanowires can incorporate proteins that retain their ability to bind their natural substrates, in this case biotin. However, the conditions of polymer deposition are constrained to aqueous buffers that are protein-compatible. Although overoxidation of Ppy occurs in these buffers, the polymer retains its electroactivity. The electrodeposition method (constant potential or potential cycling) has a marked effect on the morphology and electrochemical properties of the protein-modified conducting polymer segments, as well as on the rate of equilibration of the nanowires with biotin. Future work will explore the applications of segmented nanowires in biosensors and biomolecular assembly.

Acknowledgment. We thank Brian Kelley for assistance with T.E.M. experiments. This work was supported by NIST and by the National Science Foundation, Grant ECS-0303981.

CM0496265

(32) Smith, P. A.; Nordquist, C. D.; Jackson, T. N.; Mayer, T. S.; Martin, B. R.; Mbindyo, J.; Mallouk, T. E. *Appl. Phys. Lett.* **2000**, *77*, 1399.